# NMR Analysis of *Caenorhabditis elegans* FLP-18 Neuropeptides: Implications for NPR-1 Activation†

Aaron T. Dossey,‡,§ Vincenzina Reale,§,|| Heather Chatwin,|| Cherian Zachariah,‡ Mario deBono,⊥ Peter D. Evans,|| and Arthur S. Edison*,‡

*McKnight Brain Institute, University of Florida, 100 South Newell Drive, Building 59, Room LG-150, Gainesville, Florida 32611, The Inositide Laboratory, The Babraham Institute, Cambridge, CB2 4AT, United Kingdom, and The MRC Laboratory of Molecular Biology, Hills Road, Cambridge, CB2 2QH, United Kingdom*

*Received February 27, 2006; Revised Manuscript Received April 10, 2006*

ABSTRACT: Phe-Met-Arg-Phe-$NH_2$ (FMRFamide)-like peptides (FLPs) are the largest neuropeptide family in animals, particularly invertebrates. FLPs are characterized by a C−N-terminal gradient of decreasing amino acid conservation. Neuropeptide receptor 1 (NPR-1) is a G-protein coupled receptor (GPCR), which has been shown to be a strong regulator of foraging behavior and aggregation responses in *Caenorhabditis elegans*. Recently, ligands for NPR-1 were identified as neuropeptides coded by the precursor genes *flp-18* and *flp-21* in *C. elegans.* The *flp-18* gene encodes eight FLPs including DFDGAMPGVLRF-$NH_2$ and EMPGVLRF-$NH_2$. These peptides exhibit considerably different activities on NPR-1, with the longer one showing a lower potency. We have used nuclear magnetic resonance and biological activity to investigate structural features that may explain these activity differences. Our data demonstrate that long-range electrostatic interactions exist between N-terminal aspartates and the C-terminal penultimate arginine as well as N-terminal hydrogen-bonding interactions that form transient loops within DFDGAMPGVLRF-$NH_2$. We hypothesize that these loops, along with peptide charge, diminish the activity of this peptide on NPR-1 relative to that of EMPGVLRF-$NH_2$. These results provide some insight into the large amino acid diversity in FLPs.

Phe-Met-Arg-Phe-$NH_2$ (FMRFamide)[1] was first discovered in 1977 by Price and Greenberg as a cardioexcitatory peptide from the clam *Macrocallista nimbosa* (*1*). FMRFamide-like peptides (FLPs) are the largest family of neuropeptides found in invertebrates (*2*−*5*), but mammalian (even human) FLPs have also been identified (*6*−*9*). These peptides are characterized by a C−N-terminal gradient of decreasing sequence conservation, and most end in RF-$NH_2$. This is true when FLP peptide sequences as a whole, from within taxa, within species, or even on specific precursor proteins, are compared (*2*, *4*, *5*, *10*). The peptides, like most neuropeptides and hormones, are synthesized as part of larger precursor proteins and processed in the secretory pathway (*11*). Peptides on a particular precursor have conserved regions in the mature peptides that are often associated with receptor binding and make up a subfamily (*4*). For many neuropeptides, including FLPs, this region is the C terminus. However, other peptide families have different patterns of conservation; for example, in insect orcokinins, the N terminus is the conserved region (*12*), and in insulin, the cystine framework and other central residues are conserved (*13*). Two examples of FLP precursor proteins, flp-18 from the nematode *Caenorhabditis elegans* (*4*) and afp-1 from the nematode *Ascaris suum* (*14*) are shown in Table 1.

The first nematode FLP, AF1, was isolated from *A. suum* (*15*), and most subsequent early nematode FLP work was done on this species (*14*, *16*−*21*). FLPs are highly expressed in nematodes and thus are likely important chemical components of their anatomically simple nervous systems (*3*, *5*, *18*). In *C. elegans*, 28 different genes encoding well over 60 possible FLPs have been identified using bioinformatic approaches (*4*, *5*, *22*) and 28 of the putative processed peptides have been detected biochemically (*23*−*27*).

FLPs are involved in a wide range of biological processes that have been reviewed previously (*10*, *28*−*31*). Some of the more prominent functional studies have focused on their role in cardioexcitation (*1*), muscle contraction (*19*), modulation of the action of morphine (*32*), egg laying (*33*), and feeding behavior (*31*) in nematodes. Also, disruption of the *flp-1* gene in *C. elegans* resulted in a number of phenotypes (*34*). Although much work has been done to elucidate the activities of FLPs, the definitive biological functions of the vast majority of FLPs are still unknown.

† This work was supported by a NSF CAREER grant to A.S.E., NIH 5P41RR016105, and the Human Frontier Science Program.

* To whom correspondence should be addressed: Box 100245, Department of Biochemistry and Molecular Biology, University of Florida, Gainesville, FL 32610-0245. Telephone: 352-392-4535. Fax: 352-392-3422. E-mail: art@mbi.ufl.edu.

‡ University of Florida.

§ These authors contributed equally to this work.

|| The Babraham Institute.

⊥ The MRC Laboratory of Molecular Biology.

[1] Abbreviations: FMRFamide, Phe-Met-Arg-Phe-$NH_2$; FLP, FMRFamide-like peptide; NMR, nuclear magnetic resonance; AAA, amino acid analysis; TOCSY, total correlation spectroscopy; ROESY, rotating-frame Overhauser effect spectroscopy; $D_2O$, deuterium oxide; GPCR, G-protein coupled receptor; TC, temperature coefficient; NPR-1, neuropeptide resemblance receptor 1; *flp-n* = gene name, flp-n = precursor protein, FLP-N = peptide name.

10.1021/bi0603928 CCC: $33.50 
Published on Web 05/23/2006

Table 1: Sequence Comparison of flp-18 and afp-1 Precursor Proteins[a]

| | |
|---|---|
| flp-18 | MRFDDDTTCATTCADKLRTIEVLTGPTRFIQLYCVFFSYFSTTLTFFNYSLHH |
| afp-1 | MVELAAIAVHLFAILCISVSAEIELPDKRAQFDDSFLPYYPSSAFMDSDEAIV |
| flp-18 | LPCFSIFKIVFFVSERADQLCFFLNEKSSSQALKFLPKIESYVYSRLDMQRWS |
| afp-1 | AVPSSKPGRYYFDQVGLDAENAMSARE_____ |
| flp-18 | GVLLISLCCLLRGALAYTEPIYEIVEEDIPAEDIEVTRTNEKQDGRVFS |
| afp-1 | _____ |
| flp-18 | KR**DFDGAMPGVLRFGKRGGVWEKRESSVQKKEMPGVLRFGKRAYFDEKKSV |
| afp-1 | KRGFGDEMSMPGVLRFGKR_____GMPGVLRFGKR__ENEKKAV |
| flp-18 | PGVLRFGKRSYFDEKK*SVPGVLRFGKRDVPMDKR*EIPGVLRFGKRDYMADS |
| afp-1 | PGVLRFGKR_____GDVPGVLRFGKR_____SDMPGVLRFGKR_____ |
| flp-18 | FDKRSEVPGVLRFGKRDVPGVLRFGKRSDLEEHYAGVLLKKSVPGVLRFGRK |
| afp-1 | _____*SMPGVLRFGRR |

[a] Peptide sequences are red, and processing sites are blue. An asterisk denotes an amino acid gap in the neuropeptide, and an underline denotes a gap outside the peptide-coding region. Note that this analysis is not an alignment. The longer peptides for each precursor are underlined (*4*, *14*).

Two types of receptors for FLPs have been identified: G-protein coupled receptors (GPCRs) (*35*−*40*) and a sodium channel gated by FMRF-$NH_2$ (*41*−*43*). Other human/mammalian ion-channel receptors have been identified whose activities are modulated by FLPs, including the acid-sensing ion channels (ASICs) and epithelial $Na^+$ ion channels (ENaCs) (*8*, *44*). Neuropeptide receptor 1 (NPR-1), a GPCR that modulates feeding behavior in *C. elegans*, is activated by two subfamilies of FLPs in *C. elegans*, including the FLP-18 peptides and FLP-21 peptide (*35*). All of the FLP-18 peptides occur on the same precursor and are presumably processed and released simultaneously (*4*). The most active of these peptides is EMPGVLRF-$NH_2$; in comparison, DFDGAMPGVLRF-$NH_2$ is significantly less active (*35*). These observations motivated us to further investigate the structural properties of these peptides relative to their biological activities.

In previous studies, we have suggested that N-terminal hydrogen bonding can influence FLP activity (*45*). Structural interactions in small peptides such as FLPs are generally invisible to techniques such as X-ray crystallography, because small peptides are dynamic in solution. Also, some nuclear magnetic resonance (NMR) parameters such as nuclear Overhauser effect (NOE) correlations for distance measurements are of limited value on small peptides because of their dynamic properties in solution (*46*). However, these structural properties can modulate their activities (*45*). Although a high-resolution X-ray crystallographic structure for a FLP-18 peptide bound to NPR-1 would be extremely useful, it would not provide any information on the unbound state of the peptides. As shown below, we have identified significant structural differences between different unbound FLP-18 peptides, and this work seeks to illuminate the relationship between free ligand conformations and their activities on the NPR-1 receptor.

In the present study, we have used NMR for pH titrations, temperature titrations, and chemical-shift analyses to identify transient long-range interactions within flp-18 peptides and designed analogues. The sequence and activity diversity among these peptides have motivated us to examine the structural properties of two extreme cases. We have focused on structural features of EMPGVLRF-$NH_2$ and DFDGAMPGVLRF-$NH_2$ that may influence the activity of each peptide on NPR-1. The material presented in this paper examines the hypothesis that *local structure in the variable N-terminal regions of flp-18 peptides can modulate their binding to NPR-1*.

## EXPERIMENTAL PROCEDURES

*Peptide Synthesis.* Peptides listed in Table 2 were synthesized using standard Fmoc solid-phase methods, purified by high-performance liquid chromatography (HPLC), and verified by matrix-assisted laser desorption ionization time-of-flight (MALDI−TOF) mass spectrometry at the University of Florida Interdisciplinary Center for Biotechnology Research (UF ICBR) protein core facility.

*Peptide Sample Preparation.* Lyophilized peptides were weighed and dissolved to ~1 mM in 95% $H_2O$ and 5% deuterium oxide ($D_2O$), and the pH was adjusted to 5.5. These were aliquoted and frozen at −20 °C until being used for biological assays or NMR experiments. Small aliquots of each sample were submitted for amino acid analysis (AAA) at the UF ICBR protein core to determine more accurate concentrations. For NMR spectroscopy, the pH-stable chemical-shift standard 2,2-dimethyl-2-silapentane-5-

Table 2: Peptides Used in This Study

| name | sequence [a] | % response (n) [b] |
|---|---|---|
| peptide 1 [c] | EMPGVLRF-$NH_2$ | 100 |
| peptide 2 [d] | DFDGAMPGVLRF-$NH_2$ | 29.1 ± 5.7 (16) |
| peptide 3 | DFDGAM-$NH_2$ | 0 (3) |
| peptide 4 | DFDGEMPGVLRF-$NH_2$ | 19.0 ± 2.6 (8) |
| peptide 5 | SGSGAMPGVLRF-$NH_2$ | 118.7 ± 11.0 (4) |
| peptide 6 | AAAAAMPGVLRF-$NH_2$ | 62.4 ± 3.2 (10) |
| peptide 7 [e] | GFGDEMSMPGVLRF-$NH_2$ | 49.3 ± 16.5 (4) |
| peptide 8 | GFGDEM-$NH_2$ | 0 (3) |
| peptide 9 [f] | DFDGEMSMPGVLRF-$NH_2$ | 45.0 ± 10.5 (6) |
| peptide 10 [g] | GFGDAMPGVLRF-$NH_2$ | 104.8 ± 2.8 (8) |
| peptide 11 | PGVLRF-$NH_2$ | 43.0 ± 5.5 (14) |
| peptide 12 | PGVLRFPGVLRF-$NH_2$ | 198.1 ± 33.3 (10) |

[a] Naturally occurring sequences are underlined. The conserved PGVLRF-$NH_2$ sequence is in bold. N-Terminal "extension" sequences of native long flp-18 peptides are bold. *C. elegans*-based sequences are red, and *A. suum*-based sequences are blue. [b] Peptides ($10^{-6}$ M) were applied in 2 m pulses to *Xenopus* oocytes expressing NPR-1 215V. Results are expressed as a percent of the response to $10^{-6}$ M peptide **1** (EMPGVLRF-$NH_2$) ± SEM. [c] Most active native *C. elegans* FLP-18 peptide. [d] Longest and least active native FLP-18 peptide. [e] Longest *Ascaris* AFP-1 peptide. [f] Chimera of long FLP-18 + long AFP-1. [g] Chimera of long AFP-1 + long FLP-1.

sulfonic acid (DSS) was added to 600 μL aliquots to a final concentration of 0.17 mM.

*Biological Activity Assays: Expression in Xenopus laevis Oocytes.* Sense cRNA was prepared in vitro using the mCAP RNA capping kit (Stratagene, La Jolla, CA) from plasmid DNA containing full-length *npr-1 215V* cDNA cloned in *pcDNA3* (Invitrogen Ltd., Paisley, U.K.). RNA transcripts were synthesized using T7 RNA polymerase (Stratagene, La Jolla, CA) after linearizing the plasmid with *Apa I* (Promega UK, Southampton, U.K.) and blunting the 3′ overhangs with T4 DNA polymerase (Amersham Pharmacia Biotech, Little Chalfont, Bucks, U.K.). T7 RNA transcripts synthesized in vitro with the mCAP RNA capping kit are initiated with the 5′-7MeGpppG 5′-cap analogue. Sense cRNA was prepared in a similar manner from the GIRK1 and GIRK2 clones in *pBS-MXT* (*47*) (kindly donated by Drs. S. K. Silverman and H. A. Lester, California Institute of Technology, Pasedena, CA) after linearizing the plasmid with *Sal* I (Promega).

All experiments using *X. laevis* were carried out under a Home Office (U.K.) Project License. Stage V and VI oocytes from virgin female adult *X. laevis* were prepared using standard procedures (*35*, *48*−*50*). Oocytes were then injected with 50 ng of *npr-1* receptor sense cRNA, either alone or together with 0.5 ng each of GIRK 1 and GIRK 2 sense cRNA and incubated at 19 °C for 2−5 days. Uninjected oocytes were used as controls. Electrophysiological recordings were made from oocytes using a two-microelectrode voltage-clamp technique (*35*, *48*−*50*).

*NMR Spectroscopy.* NMR data were collected at 600 MHz on a Bruker Advance (DRX)-600 console in a 14.1 T magnet equipped with a 5 mm TXI Z-Gradient CryoProbe. Unless otherwise stated, all NMR experiments were collected at 288 K, and spectra were collected with a 6600 Hz spectral width and referenced by setting the methyl proton resonance peak from DSS protons to 0.0 ppm. The $^1$H carrier frequency was centered on water, which was reduced using a WATERGATE sequence (*51*) or presaturation. Two-dimensional total correlation spectroscopy (TOCSY) (*52*) experiments were collected using a DIPSI-2 mixing sequence with a 60 ms mixing time. Two-dimensional rotating-frame Overhauser effect spectroscopy (ROESY) (*53*) experiments were collected using a 2.27 kHz cw field spinlock applied for 250 ms.

Processing of 1D NMR spectra and creation of stack plots of pH and temperature titrations was done using Bruker XWINNMR and XWINPLOT version 4.0 software. Two-dimensional NMR datasets were processed with NMRPipe (*54*) using standard methods: removing residual water by deconvolution, multiplying the data with a squared cosine function, zero filling, Fourier transformation, and phase correction. Data were analyzed and assigned with NMRView (*55*) using standard $^1$H-based methods (*56*).

One-dimensional pH-titration experiments were performed for all peptides in Table 2 that contain aspartate and/or glutamate residue(s), as well as PGVLRF-$NH_2$ and SGSGAMPGVLRF-$NH_2$ as controls. One-dimensional NMR spectra were collected at increments of about 0.2 pH units from 5.5 to 1.9 by adding 1−3 μL of 0.01−0.1 M HCl for each pH value. p$K_a$ values and effective populations ($c$ in eq 1) of pH-dependent resonance peaks were calculated using Origin 7.0 software and a modified version of the Henderson−Hasselbach equation below as previously described (*57*)

$$\delta(\mathrm{pH}) = \sum_{i=1}^{j} \frac{c_i(\delta_a - \delta_b) \times 10^{\mathrm{p}K_{ai}-\mathrm{pH}}}{1 + 10^{\mathrm{p}K_{ai}-\mathrm{pH}}} \qquad \sum_{i=1}^{j} c_i = 1$$

$$j = 1 \text{ or } 2$$

where $\delta$(pH) is the experimental chemical shift, $\delta_b$ is the chemical shift at the least acidic condition, $\delta_a$ is the chemical shift at the more acidic condition, p$K_{ai}$ is the negative common log of the acid/base equilibrium constant for the $i$th titration event, and $c_i$ is the contribution of the $i$th titration event to the total pH dependence of the chemical shift.

One-dimensional NMR temperature titrations were collected on a standard TXI probe at 5 K increments from 278 to 328 K and then ramped back to 278 K to check for sample integrity. The temperature for each experiment was calibrated using methanol (for 278.15−298.15 K) and ethylene glycol (for 308.15−328.15 K), and the corrected temperatures were used for the determination of all temperature coefficients (TCs).

## RESULTS

*Peptide Design Rationale and Physiological Responses.* Three major considerations have motivated this study. First, we have been intrigued for some time by the amino acid diversity in FLPs (*2*, *10*, *14*−*16*, *45*, *58*, *59*). In particular, as described above, FLPs display patterns of decreasing amino acid conservation from the C to N termini, and the comparison of the *C. elegans flp-18* (*4*) and *A. suum afp-1* (*14*) genes suggests that the longer peptides produced by

these genes are unique (see Table 1). Second, the activity at NPR-1 of the long FLP-18 peptide, DFDGAMPGVLRF-$NH_2$, is significantly lower than the shorter EMPGVLRF-$NH_2$ (*35*). Finally, in previous work on FLPs from mollusks, we found that different amino acid substitutions significantly changed the conformations of the peptides (*45*, *58*) and that these conformational differences are correlated with their differences in activity (*60*).

In designing the peptides for this study, we considered several possibilities to explain the difference in NPR-1 activity between two native FLP-18 peptides, EMPGVLRF-$NH_2$ and DFDGAMPGVLRF-$NH_2$: first, the N terminus could have intrinsic activity or act as a competitive inhibitor; second, a glutamic acid might be required in a position corresponding to the first residue of the more active EMPGVLRF-$NH_2$; third, the added bulk because of the extra amino acids could prevent the active portion of the peptide from efficiently binding to NPR-1; fourth, the N-terminal extension of DFDGAMPGVLRF-$NH_2$ could be involved in structural interactions that cause it to be less potent on NPR-1 than EMPGVLRF-$NH_2$. To address these possibilities, two native FLP-18 peptides and a range of substituted and derived analogues (Table 2) were tested for their ability to activate the NPR-1 215V receptor expressed as described in the Experimental Procedures. In the following, we use the term "activity" to indicate the magnitude of the potassium current evoked by a $10^{-6}$ M pulse of peptide as a percentage of the response of the same oocyte to a $10^{-6}$ M control pulse of peptide 1 (EMPGVLRF-$NH_2$). We will refer to peptides by their peptide number shown in Table 2.

It was observed that that the long native FLP-18 peptide **2** was much less effective than the shorter FLP-18 peptide **1** at activating the receptor (Table 2), confirming previous observations (*35*). To test if the N terminus of peptide **2** could have intrinsic activity or act as a competitive inhibitor, we designed and analyzed the effect of peptide **3**. This peptide had no intrinsic activity on the receptor (Table 2) and did not block the effects of 1 $\mu$M pulses of peptide **1** ($n = 3$) (data not shown). To test the possibility that a glutamic acid might be required in a position corresponding to the first residue peptide **1**, we examined peptide **4**, where a glutamic acid residue is substituted for alanine at position 5 in peptide **2**. However, this substitution did not improve and, in fact, weakened the effectiveness of the long peptide. It also seemed possible that the added bulk of peptide **2** because of the extra amino acids could be preventing access to the NPR-1-binding site. Thus, we analyzed peptides **5** and **6**. Peptide **5** was designed to eliminate any potential structure in the N terminus based on commonly used flexible linker sequences in fusion protein constructs (pET fusion constructs, Novagen, Inc.). The N terminus of peptide **6** was designed to induce a nascent helical structure in the same region (*61*, *62*). It can be seen that peptide **5** completely restored activity compared to peptide **2**, while peptide **6** only partially restored activity in comparison with the short native peptide.

As shown in Table 1, the longest native peptide from *afp-1* in *A. suum* (*19*), peptide **7**, is two amino acids longer than the corresponding longest peptide from the *C. elegans flp-18* gene (*4*), peptide **2**. Thus, we also synthesized and tested peptide **7**, as well as its N terminus, peptide **8**. Peptide **7** was slightly more effective than peptide **2**. However, the short N-terminal peptide sequence was again inactive (Table 2) and did not block the effects of 1 $\mu$M pulses of peptide **1** ($n = 3$) (data not shown). In addition, we also made chimeras of the long *C. elegans* and *A. suum* sequences, peptides **9** and **10**. Peptide **9**, in which two extra amino acids (SM) are introduced into the center of peptide **4** to give it the same number of amino acids as peptide **7**, showed similar activity to that of the long native *Ascaris* peptide itself, GFG-DEMSMPGVLRF-$NH_2$. However, peptide **10** showed similar activity to that of peptide **1**.

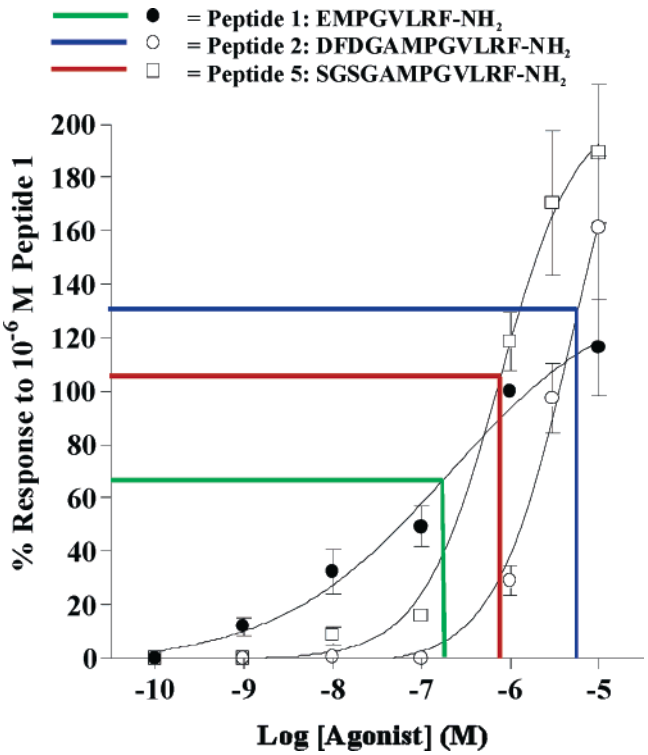


FIGURE 1: Dose−response curves of select FLP-18 peptides. Peptides were applied to *Xenopus* oocytes expressing NPR-1 215V, and the responses from inward rectifying $K^+$ channels were recorded and normalized to the response of peptide **1** (EMPGVLRF-$NH_2$) at $10^{-6}$ M. (●) Peptide **1** (EMPGVLRF-$NH_2$) ($EC_{50} = 10^{-6.80}$ M), (□) peptide **5** (SGSGAMPGVLRF-$NH_2$) ($EC_{50} = 10^{-6.12}$ M), and (○) peptide **2** (DFDGAMPGVLRF-$NH_2$) ($EC_{50} = 10^{-5.28}$ M). Three measurements at each peptide concentration were obtained, and results are shown ± the standard error of the mean (SEM).

As shown later, our results indicate that the conserved C-terminal PGVLRF-$NH_2$ is largely unstructured in solution. Thus, we tested peptide **11** and also peptide **12**, in which the conserved sequence was duplicated. The activity of peptide **11** was less than that of peptide **1** and similar to that of peptides **7** and **9**. In comparison to peptides **1** and **5**, the reduced activity of peptide **11** could indicate that methionine preceding proline is important for activity. However, the C-terminal duplicated peptide with no methionine was approximately twice as active as peptide **1**.

To further investigate the effects of changing the structure of the N-terminal sequence of the *C. elegans* long FLP-18 peptide, we determined full dose−response curves for peptides **1**, **2**, and **5** (Figure 1).

From Figure 1, both peptides **2** and **5** are less potent compared to peptide **1**. This suggests that elimination of the structure at the N terminus of peptide **2** can increase its potency on the receptor. Also, peptides **2** and **5** are more efficacious at higher concentrations than peptide **1**, suggest-

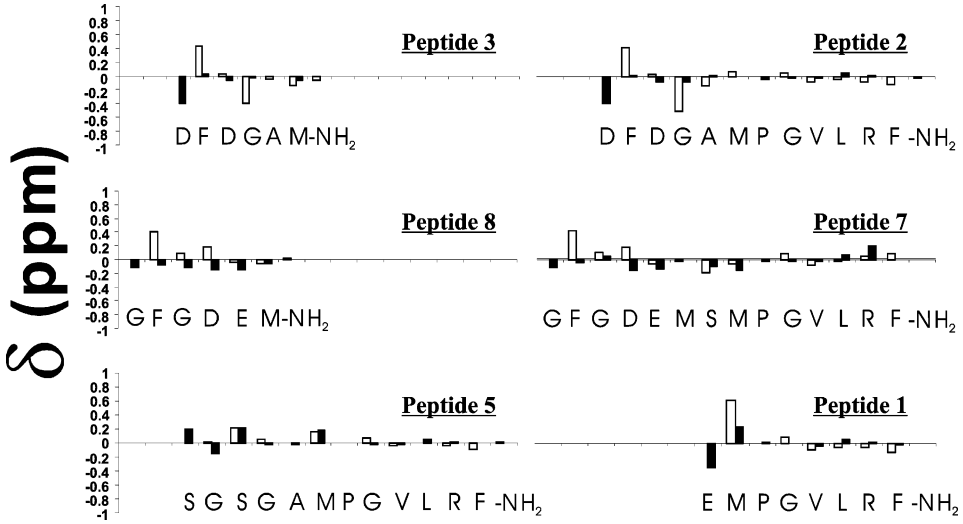


FIGURE 2: NMR chemical-shift deviations from random-coil values. Experimental chemical shifts at pH ~2.3 were subtracted from sequence-corrected random-coil values (*64*, *65*). Filled and open bars represent α and amide protons, respectively.

ing that longer peptides might be more efficacious on NPR-1 than shorter peptides.

*NMR Chemical Shifts Reveal Regions of flp-18 Peptides with Significant Structure.* Chemical shifts are extremely sensitive to molecular and electronic environments and thus provide unique atomic probes in molecules. Specifically, in peptides and proteins, chemical shifts of many nuclei along the polypeptide backbone have been shown to be dependent upon the secondary structure (*46*, *63*−*68*). Thus, the first step in NMR analysis is the assignment of resonance peaks in spectra to atoms in the molecule. For all peptides in Table 2, nearly complete NMR resonance assignments were made using standard two-dimensional $^1$H-based methods (*56*) (see Table S2 in the Supporting Information).

Short, linear peptides are often very dynamic, lack a 3D hydrophobic core, and interconvert rapidly between many different conformations. Despite this inherent flexibility, numerous studies have demonstrated that regions of short peptides can be highly populated in specific types of secondary structure (*69*−*72*). A fundamental hypothesis of this study is that differences in local structure of variable N termini of free FLPs could partially explain differences in their potencies on receptors.

To compare chemical shifts from one peptide to another and to identify regions that contain significant populations of secondary structure, it is useful to compare experimental chemical shifts to random-coil values (*64*−*66*, *68*). Figure 2 plots the difference between experimental and random-coil values for some of the peptides analyzed in this study. The white and black bars represent deviations from random-coil values for amide and α protons, respectively, and the magnitude of the deviations reflects the population of the local structure along the backbone of the peptides (*64*, *68*). All data were compared to random-coil values at pH 2.3.

Several features in Figure 2 are worth noting. First, the chemical shifts of residues in the conserved PGVLRF-$NH_2$ regions of each peptide are close to random-coil values and rather similar among all of the peptides examined. This suggests that this conserved sequence is unstructured in solution and that flexibility is important for binding to NPR-1. This flexibility may help the ligand diffuse/maneuver more effectively into a binding pocket on the receptor. Second, the N-terminal extension of peptide **2** shows significant deviation from random-coil values. In particular, the G4 amide proton has a very large deviation, suggesting significant structure. Third, the chemical-shift deviations of amide and α protons of peptides **3** and **8** are nearly identical to the corresponding regions of the full-length peptides **2** and **7**, respectively. This indicates that these N-terminal extensions are behaving as independent structural units. Finally, peptide **5**, designed to lack the N-terminal structure, indeed shows a consistent very small deviation from random-coil values in its first five residues.

*pH Dependence of Amide Proton Chemical Shifts Reveals Regions of flp-18 Peptides with Significant Structure.* The sensitivity of NMR chemical shifts to electronic structure and hydrogen bonding makes them ideal probes of longer range interactions with titratable side chains. NMR studies of peptides that utilize amide protons often need to be conducted below pH ~6 to prevent amide proton exchange (*56*, *73*). When the pH is varied from about 5.5 to 2, both aspartic and glutamic acid side chains will be converted from negatively charged and deprotonated to neutral and protonated. These different charge states of the carboxylate groups will produce changes in the electronic environment in interacting atoms proportional to $1/R^3$, where $R$ is the distance between the charged group and chemical-shift probe. Backbone amide resonances are particularly sensitive to interactions such as hydrogen bonding (*57*, *66*) and thus provide ideal probes of long-range interactions with side-chain carboxylates. This phenomenon provides a powerful mechanism to study long-range hydrogen-bonding and salt-bridge interactions in small peptides (*45*, *73*, *74*).

Many of the FLP-18 peptides contain aspartic or glutamic acids; therefore, we performed 1D NMR pH-titration experiments on all peptides in Table 2 containing these residues and, as controls, on peptides **5** and **11**, neither of which showed any pH dependence in the proton chemical shifts. Stack plots of the amide region for a representative set of peptides are shown in Figure 3.

No chemical shifts in peptide **5** (Figures 3E and 4E) or peptide **11** (data not shown) have any pH dependence, demonstrating that backbone amide proton chemical shifts are not intrinsically pH-dependent in this pH range. Second,

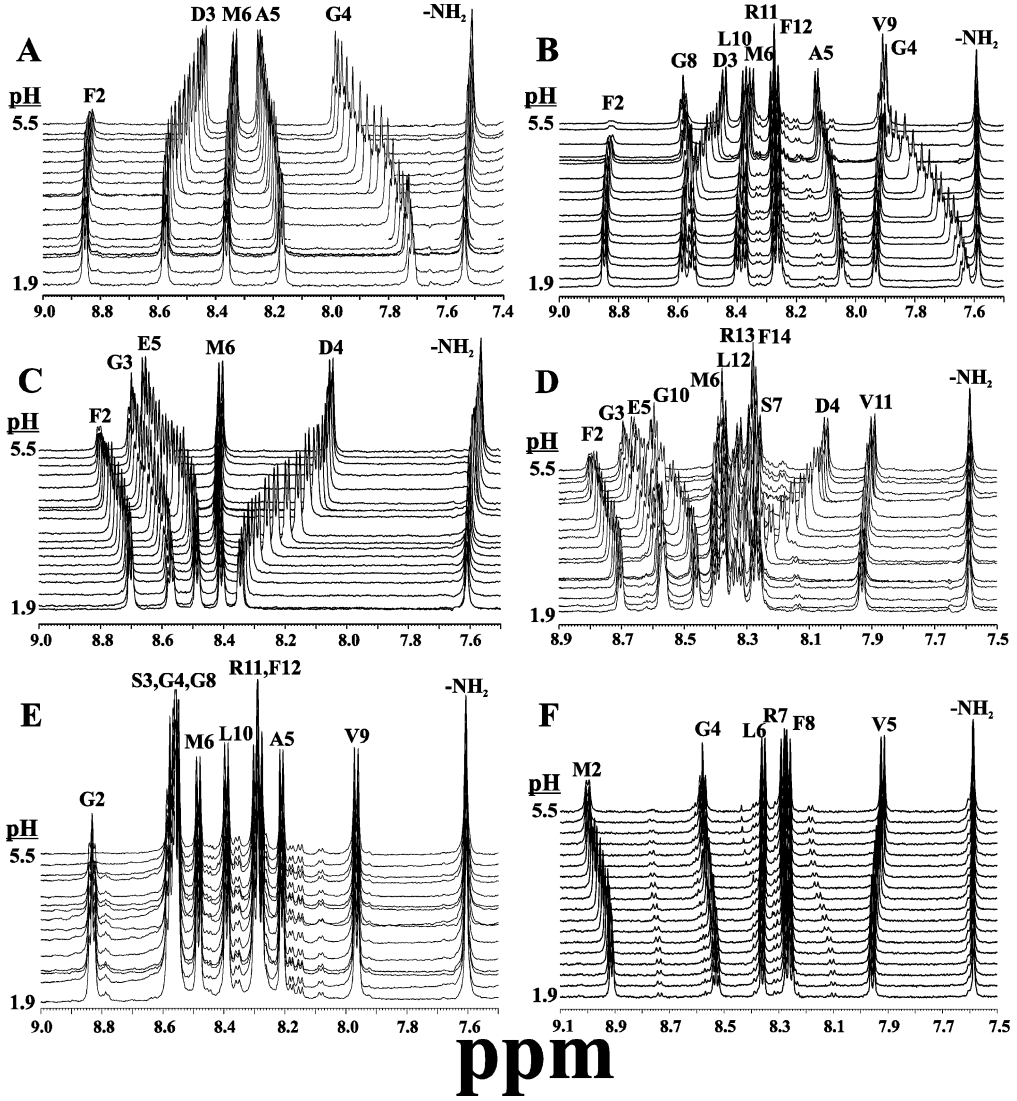


FIGURE 3: Amide region of one-dimensional NMR data, collected as a function of the pH from about 1.9 to 5.5. Peaks are labeled with their assigned amino acids, and the panels correspond to the following peptides: (A) peptide **3**, DFDGAM-$NH_2$; (B) peptide **2**, DFDGAMPGVLRF-$NH_2$; (C) peptide **8**, GFGDEM-$NH_2$; (D) peptide **7**, GFGDEMSMPGVLRF-$NH_2$; (E) peptide **5**, SGSGAMPGVLRF-$NH_2$; and (F) peptide **1**, EMPGVLRF-$NH_2$. pH-dependent interactions are summarized in Figure 5, and complete p$K_a$ analyses are provided in the Supporting Information.

several resonances in other peptides have large pH-dependent shifts. To our knowledge, no systematic study has been undertaken to identify the maximum change in the chemical shift of backbone amide protons as a function of pH, but Wüthrich and co-workers showed that a chemical shift in a small protein with a well-defined (~70−90% populated) hydrogen bond between an aspartic acid side chain and a backbone amide proton led to a change of 1.45 ppm over the titratable range of the aspartic acid (*75*). Thus, in Figure 3, some amide proton resonances of nontitratable amino acids have pH-dependent shifts that are characteristic of significant hydrogen-bond interactions. Others have smaller pH-dependent changes, suggesting either more transient dynamic interactions or much longer and weaker hydrogen bonds. In contrast, several resonances in peptides with titratable groups show little or no pH dependence, showing that these effects are relatively specific. Next, the spectra from the N-terminal truncated peptides **3** and **8** are highly dependent upon pH and are nearly perfect subsets of the same regions in their full-length counterparts. Consistent with chemical-shift data in Figure 2, this demonstrates that the N-terminal extensions of peptides **2** and **7** behave as independent structural units. The extensions also do not interact significantly with the more C-terminal backbone atoms, which show relatively little pH dependence, indicating that the conserved C termini are less structured than the N-terminal extensions.

*pH Dependence of Arginine Side Chains Reveals Long-Range Interactions.* The penultimate arginine residue is highly conserved and found in the same position in all FLPs. This arginine is at least seven residues away from any carboxyl groups; therefore, we were surprised to find in several FLP-18 peptides that its $\epsilon$ proton (Arg H$^{\epsilon}$) is pH-dependent (Figure 4).

Peptide **5** demonstrates that there is no intrinsic pH dependence of Arg H$^{\epsilon}$ over the pH range investigated, and we conclude that in other peptides there are long-range interactions between the Arg and the N-terminal carboxylates. Such an interaction would indicate a noncovalent ring structure. These interactions show up in most of the FLP-18 analogues having N-terminal carboxyl side chains and, at first glance, do not appear to relate to the activity of the peptides (Table 2). For example, peptide **1** (one of the more

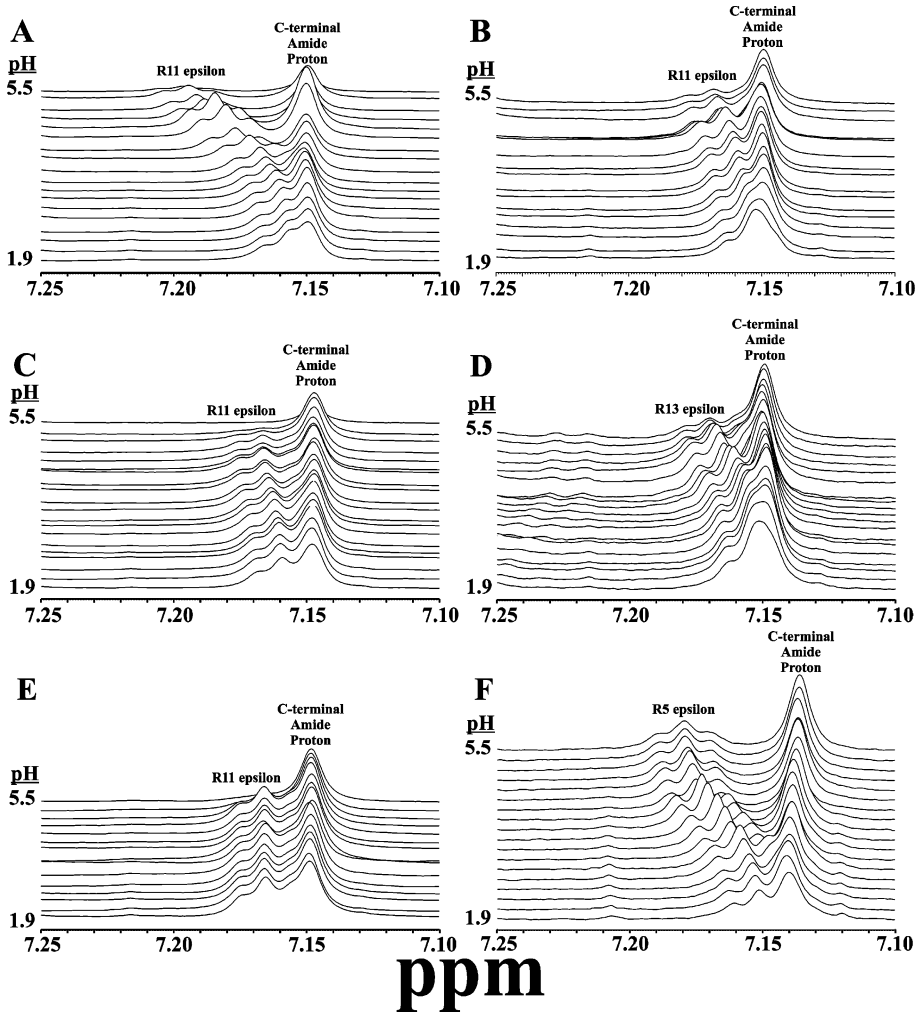


FIGURE 4: Arg $H^{\epsilon}$ region of one-dimensional NMR data, collected as a function of the pH from 1.9 to 5.5. These long-range interactions on the penultimate C-terminal Arg result from the titratable carboxylate groups on the N termini. pH-dependent interactions are summarized in Figure 5, and complete p$K_a$ analyses are provided in the Supporting Information. (A) Peptide **4**, DFDGEMPGVLRF-$NH_2$; (B) peptide **2**, DFDGAMPGVLRF-$NH_2$; (C) peptide **10**, GFGDAMPGVLRF-$NH_2$; (D) peptide **7**, GFGDEMSMPGVLRF-$NH_2$; (E) peptide **5**, SGSGAMPVLRF-$NH_2$; and (F) peptide **1**, EMPGVLRF-$NH_2$.

active peptides) has nearly the same Arg $H^{\epsilon}$ pH dependence as peptide **4** (the least active PGVLRF-$NH_2$-containing peptide examined). Moreover, peptide **10**, with a similar activity to peptide **1**, has nearly no Arg $H^{\epsilon}$ pH dependence. Thus, the Arg interaction with acidic residues alone is not sufficient to explain the difference in activity among the FLP-18 analogues tested.

*Quantitative Determination of p$K_a$ Reveals Multiple Interactions.* Several of the peptides in Table 2 have more than one carboxylate; therefore, it is not always obvious which is responsible for the pH dependence of a particular resonance. If the titrating groups have distinct p$K_a$ values, then it should be possible to determine the contribution of each carboxylate on each titrating resonance using eq 1. Every peak that exhibited pH-dependent chemical shifts was fitted using first one, then two, and then three p$K_a$ values. In all cases, we used the minimum number of interacting p$K_a$ values to get a good quality of fit and maximum linear regression coefficient ($R^2$) to the experimental data. In the peptides with three titrating groups, inclusion of three interacting groups in the calculation did not improve the fits more so than including only two.

The complete table of relative p$K_a$ contributions (*c* from eq 1) and p$K_a$ values is provided in Table S1 in the Supporting Information, and the interactions are represented graphically in Figure 5. As we discuss below, the interactions between titrating groups and resonances in these peptides is rather complicated and dynamic. The data presented here illustrate that, although there is a heterogeneous ensemble of hydrogen-bonding interactions between various backbone amide protons, certain ones are prominent.

Using the p$K_a$ values calculated for the pH-dependent resonances for the peptides in this study, we can assign most hydrogen-bonding interactions between titrating carboxyl side chains and either backbone amide or Arg $H^{\epsilon}$ protons. Figure 5 also illustrates the relative strength of these interactions. The most significant interaction (the largest shift from a long-range interaction) is from a hydrogen bond between the D1 carboxylate and G4 amide in all peptides containing the N-terminal DFDG sequence. It contributes 40% to the observed titration of the G4 amide in peptides **2** and **3** and 55% to that of peptide **4** (see the Supporting Information). The calculated p$K_a$ of D1 (~3.0) is significantly lower than that of D3 (~4.0), indicating that D1 is likely interacting with the positively charged amino terminus and stabilizing its negative charge. This is also seen in peptide **1**, because E1 also has an unusually low p$K_a$ (~3.5). Additional support for this p$K_a$ assignment comes from the p$K_a$ of the α protons

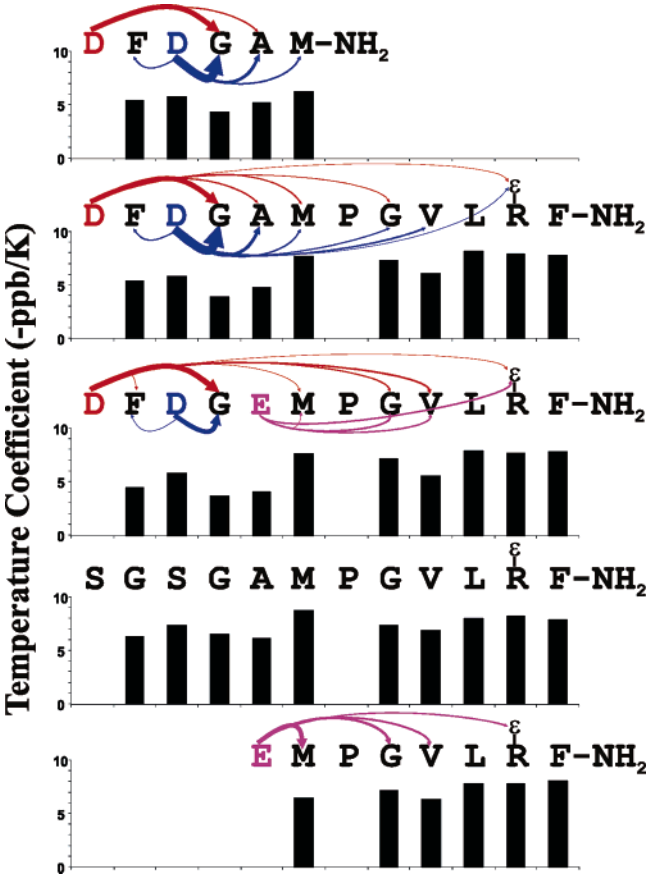


FIGURE 5: Proposed hydrogen-bonding interactions between backbone amide protons and carboxyl side chains: peptide **3**, DFDGAM-$NH_2$; peptide **2**, DFDGAMPGVLRF-$NH_2$; peptide **4**, DFDGEMPGVLRF-$NH_2$; peptide **5**, SGSGAMPGVLRF-$NH_2$; and peptide **2**, EMPGVLRF-$NH_2$. Each hydrogen-bond acceptor residue is color-coded to match the arrows leading from it to its hydrogen-bond donors. The arrow widths are proportional to the relative extent to which that particular interaction affects the chemical shift of the amide proton at the point end of the arrow. The bar plots show the TC of the backbone amide proton resonances.

of D1 and D3 of peptide **3** and D1 of peptide **2**, which are 3.23, 4.09, and 2.97, respectively (see the Supporting Information).

The interactions observed from pH titrations of peptides beginning in GFGD are different from and less substantial than those beginning in DFDG. For example, the largest pH-dependent chemical-shift change of the amide proton of a nonacidic amino acid for peptide **7** is ~0.12 ppm (G3), whereas G4 in peptide **2** is ~0.28 ppm. Also, the arginine side chain of peptides **7** and **9** show a rather small chemical-shift change in the pH titration (Figure 4D) compared the same resonance for peptides **2** and **4**. Additionally, the D4 side chain of GFGD containing peptides seems to interact primarily with backbone amides N-terminal to it (see Table S1 in the Supporting Information). This is a different conformation entirely than that observed in DFDG-containing peptides, where D1 has a substantial interaction with G4.

*Temperature Dependence of Amide Chemical Shifts Corroborates Regions with Hydrogen Bonding.* Although complicated and often over-interpreted, the temperature dependence of amide proton chemical shifts in polypeptides can be associated with hydrogen bonding (*46*, *76*). Additionally, some peptides analyzed here lacked carboxyl side chains; therefore, pH titration results were not valid in determining

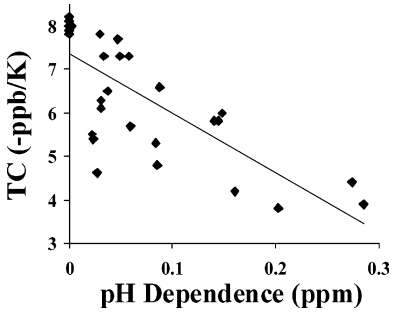


FIGURE 6: Relationship between TCs and pH dependence of the chemical shift among backbone amide protons. Plotted here is the chemical-shift change with pH versus the temperature for backbone amide resonances. $R^2$ for the linear fit is 0.58. All data from peptides **1**−**4** are represented.

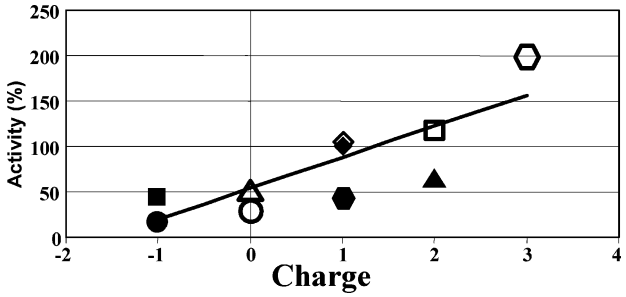


FIGURE 7: Relationship between the overall peptide charge and the activity on the NPR-1 receptor. The overall peptide charge at neutral pH is plotted against the activity for all of the peptides analyzed in this study. For the linear fit, $R^2 = 0.67$. (●) **4**, (○) **2**, (■) **9**, (□) **5**, (▲) **6**, (△) **7**, (◆) **1**, (◇) **10**, (⬢) **11**, and (⬡) **12** (numbers correspond to peptide numbers in Table 2).

possible structural interactions in these peptides. We therefore measured TCs for several relevant peptides (Figure 5). A rough guideline to interpreting TCs is that an absolute value of less than 4 indicates an internal hydrogen bond, values between 4 and 6 indicate weak hydrogen bonding, and values greater than 6 are not involved in hydrogen bonding (*46*, *76*, *77*). The magnitudes of the TCs for all amide protons in this study are inversely correlated with the magnitude of chemical-shift pH dependence for those resonances (Figure 6), which is consistent with hydrogen-bonding interactions as described above.

*Overall Peptide Charge Is Correlated with Activity on NPR-1.* The experimental data presented above demonstrate that acidic residues in the N-terminal regions of FLP-18 peptides can interact with numerous amide protons and the conserved penultimate Arg. Although there are many additional factors influencing activity as addressed below, there appears to be a qualitative relationship between their charge properties (particularly of the N terminus) and activities on NPR-1. This relationship is demonstrated in Figure 7, where the overall net charge at pH 7 of the entire peptide is plotted against its activity on NPR-1.

## DISCUSSION

The goal of this work has been to determine the conformational properties of unbound FLP-18 neuropeptides from *C. elegans* and how these may affect their potencies on NPR-1. The starting point for this study was the knowledge that two of the peptides encoded by the *flp-18* gene have significantly different potencies on NPR-1 (*35*). The major findings reported above can be summarized as follows:

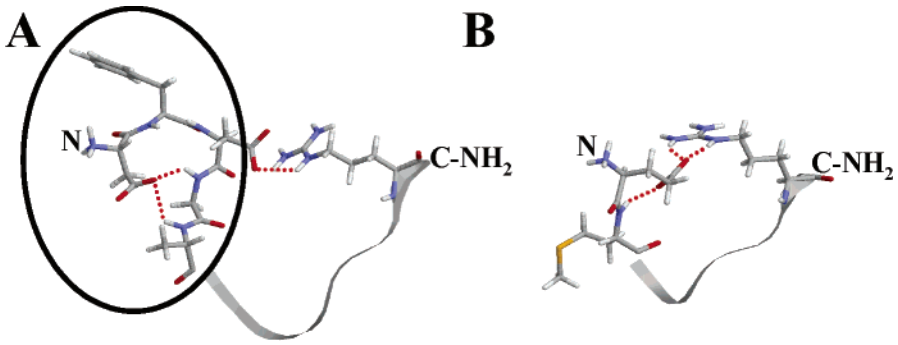


FIGURE 8: Model of interactions thought to be occurring within native FLP-18 peptides. This figure shows the most significant hydrogen-bonding interactions supported by NMR data. (A) For DFDGAMPGVLRF-$NH_2$, hydrogen-bonds between the D1 side-chain carboxylate and G4/A5 backbone amide protons as well as hydrogen-bonding/ionic interaction between the D3 side chain are represented by red dashed lines. The N-terminal loop structure implicated in inhibiting binding to NPR-1 is circled in black. (B) EMPGVLRF-$NH_2$ is shown with the most significant hydrogen-bonding and ionic interactions for which we have evidence. Notice that it has no N-terminal loop, in contrast to DFDGAMPGVLRF-$NH_2$. Also, the same unstructured region for both peptides is shown in ribbon view. The N and C termini are also labeled on both peptides.

- The backbone of the conserved PGVLRF-$NH_2$ is predominantly unstructured.
- DFDG forms a structural loop stabilized by hydrogen bonding.
- Another loop forms when N-terminal acidic residue(s) interact with the conserved C-terminal penultimate arginine side chain.
- The DFDG loop interacts with the second loop to form a dynamic bicyclic structure that might influence binding to NPR-1.
- Charge also affects the activity of FLP-18 peptides on NPR-1.

*The Backbone Structure of the Conserved PGVLRF-$NH_2$ Is Predominantly Unstructured.* All NMR structural parameters measured in this study for the PGVLRF-$NH_2$ region of FLP-18 peptides indicate that the peptide backbone of this conserved sequence is predominantly unstructured. The only significant evidence for any kind of structural motif is the interaction between the conserved penultimate arginine side chain and acidic residues in the N termini. These results suggest that the primary receptor-binding region of FLP-18 peptides is highly flexible before interacting with NPR-1.

*DFDG Forms a Structural Loop Stabilized by Hydrogen Bonding.* We observe transient hydrogen-bonding and ionic interactions within FLP-18 peptides beginning in the sequence DFDG. Specifically, acidic residues in the variable N termini form substantial hydrogen bonds to backbone amides N-terminal to the conserved proline (Figures 5 and 8).

In the DFDG-containing peptides, G4 has the smallest TC of all amides in the study; this is characteristic of involvement in a significant hydrogen-bonding interaction (*46*, *76*, *78*). This phenomenon is particularly prominent in peptide **4**, where the D1 p$K_a$ rather than that of D3 is the most significant contributor to the G4 amide proton titration. It is also the least active PGVLRF-$NH_2$-containing peptide tested. Also, weak ROESY peaks were observed between D1 $\beta$ protons and G4 $\alpha$ protons in both peptides **2** and **3** (data not shown). This further corroborates the pH titration results that indicate significant long-range hydrogen bonding between the D1 side chain and G4 backbone amide proton of peptides beginning with DFDG. In contrast, the N-terminal SGSG region of peptide **5** is unstructured on the basis of our NMR results and is one of the most active peptides analyzed.

*The DFDG Loop May Interact with the Second Loop To Form a Dynamic Bicyclic Structure, Which Reduces Binding to NPR-1.* There is no direct or simple correlation between the activity data and any one set of NMR data. However, the two carboxylate residues in peptides **2** and **4** allow for both the N-terminal loops as well as the ionic interaction between the conserved arginine and aspartates (Figure 8A). The increased activities of peptides **7** and **9**, along with their apparent weaker interaction between the penultimate arginine and acidic residues relative to peptides **2** and **4**, illustrate that the residues SM inserted in the middle of these peptides can interfere with loop formation between the N and C termini. FLP-18 peptides are short and flexible, and both loop interactions are likely dynamic. However, there is a possibility that the bulk of the N-terminal loop in DFDG-containing peptides is brought into proximity of the conserved receptor-binding region by the action of the second loop involving the penultimate arginine. We propose that this bicyclic structure reduces binding to NPR-1.

*Charge Is Also Important in Determining the Activity of flp-18 Peptides on NPR-1.* There is a significant correlation between charge and activity such that more positively charged peptides tend to activate NPR-1 better than more negatively charged ones. Interestingly, the vast majority of predicted FLPs in *C. elegans* tend to be positively charged (*4*), including the peptide encoded by *flp-21*, which has an overall charge of +3 and is active on both naturally occurring isoforms of NPR-1 (215F and 215V). However, peptides **4** and **9** have the same charge but different activities on NPR-1. The acidic residues of peptides **4** and **9** differ substantially in their interaction with the C-terminal arginine. This is likely due to the insertion of the residues SM in the middle of peptide **9**. Thus, the N-terminal DFDG loop in peptide **9** does not interact well with the penultimate arginine, whereas that of peptide **4** does. This further supports the bicyclic model and the affect of a two-loop conformation on the activities of DFDG-containing peptides.

Peptides **6** and **12** were often outliers in our attempts to correlate specific NMR data parameters to activity results. Peptide **6** was designed to possess a helix in the N terminus, and we predicted reduced binding to NPR-1, resulting in activity similar to that of peptide **2**. This prediction was incorrect, and peptide **6** had more activity than peptide **2**. However, with no carboxylates, peptide **6** lacks the ability

to form side-chain-mediated hydrogen-bonding loops, which our model suggests should give it an activity more like that of peptides **1** and **5**. Thus, the activity of peptide **6** (intermediate between peptides **1** and **2**) suggests that other properties of its structure modulate its potency.

Peptide **12** unexpectedly had nearly exactly twice the activity of peptide **1**. It is composed of two copies of the conserved PGVLRF sequence that is responsible for FLP-18 activity on NPR-1. Previous studies on FLP receptors show that the C-terminal amide group is necessary for activity (*40*); therefore, it is extremely unlikely that the C-terminal PGVLRF in peptide **12** can interact with the active site of NPR-1. However, this peptide is also the most positively charged of all among those tested. This is consistent with our observation that the charge of a peptide influences its activity on NPR-1.

Both native FLP-18 peptides in this study, DFDGAMPGVLRF-$NH_2$ and EMPGVLRF-$NH_2$, differ in both potency and efficacy. We have shown that the N-terminal structure, peptide charge, loop formation, and backbone flexibility in PGVLRF-$NH_2$ all modulate the activity of FLP-18 peptides on NPR-1. One interesting feature of the dose−response curves in Figure 1 is that the two longer peptides have a larger maximal response and a steeper linear portion than the shorter peptide. This suggests that the native peptides could induce different configurations of the NPR-1 receptor with different abilities to couple the G-protein pathway under study and perhaps other additional second messenger pathways as yet untested (*79*−*82*). Both the *A. suum* and *C. elegans* long peptides have been isolated (*19*, *23*), demonstrating that these exist in vivo. However, other studies (*83*, *84*) have shown that many peptide degradation products can also be found in cells. Perhaps multiple forms of FLP-18 peptides could shape the behavioral response to NPR-1 activity in a way that could not be achieved by any one peptide alone. It is possible that the ensemble of peptides functions as a bouquet to achieve a unique, beneficial, fine-tuned response (*2*, *45*).

## ACKNOWLEDGMENT

Peptides were synthesized and purified by Alfred Chung, and amino acid analyses were done by Scott McClung in the ICBR Protein Core facility at the University of Florida. We thank Jim Rocca and Dan Plant in the McKnight Brain Institute AMRIS facility for excellent NMR support. We thank Omjoy Ganesh for writing a program used to implement published sequence-dependent corrections to the random-coil chemical shifts. A. S. E. thanks Tony Stretton for many helpful and pleasant discussions. A. T. D. and C. Z. did the NMR data analysis. V. R. did electrophysiological activity measurements. H. C. prepared cDNA and cRNA for the NPR-1 receptor, which was supplied by M. deB. A. T. D., P. D. E., and A. S. E. formulated the hypotheses, interpreted the results, and developed the conclusions.

## NOTE ADDED AFTER ASAP PUBLICATION

The footnote in Table 1 has been revised from the version published ASAP May 23, 2006; the correct version was published ASAP June 6, 2006.

## SUPPORTING INFORMATION AVAILABLE

Table S1, calculated p$K_a$ values for all pH-dependent resonances in all peptides examined by NMR pH titration and calculated proportion contributions for each p$K_a$ to each pH-dependent resonance; Table S2, $^1$H NMR chemical-shift assignments for all peptides examined by NMR. This material is available free of charge via the Internet at http://pubs.acs.org.

## REFERENCES

1. Price, D. A., Greenberg, M. J. (1977) Structure of a molluscan cardioexcitatory neuropeptide, *Science 197*, 670−671.
2. Greenberg, M. J., and Price, D. A. (1992) Relationships among the FMRFamide-like peptides, *Prog. Brain Res. 92*, 25−37.
3. Li, C., Nelson, L. S., Kim, K., Nathoo, A., and Hart, A. C. (1999) Neuropeptide gene families in the nematode *Caenorhabditis elegans*, *Ann. N.Y. Acad. Sci. 897*, 239−252.
4. Li, C., Kim, K., and Nelson, L. S. (1999) FMRFamide-related neuropeptide gene family in *Caenorhabditis elegans*, *Brain Res. 848*, 26−34.
5. McVeigh, P., Leech, S., Mair, G. R., Marks, N. J., Geary, T. G., and Maule, A. G. (2005) Analysis of FMRFamide-like peptide (FLP) diversity in phylum Nematoda, *Int. J. Parasitol. 35*, 1043−1060.
6. Vilim, F. S., Aarnisalo, A. A., Nieminen, M. L., Lintunen, M., Karlstedt, K., Kontinen, V. K., Kalso, E., States, B., Panula, P., and Ziff, E. (1999) Gene for pain modulatory neuropeptide NPFF: Induction in spinal cord by noxious stimuli, *Mol. Pharmacol. 55*, 804−811.
7. Perry, S. J., Yi-Kung Huang, E., Cronk, D., Bagust, J., Sharma, R., Walker, R. J., Wilson, S., and Burke, J. F. (1997) A human gene encoding morphine modulating peptides related to NPFF and FMRFamide, *FEBS Lett. 409*, 426−430.
8. Perry, S. J., Straub, V. A., Schofield, M. G., Burke, J. F., and Benjamin, P. R. (2001) Neuronal expression of an FMRFamide-gated $Na^+$ channel and its modulation by acid pH, *J. Neurosci. 21*, 5559−5567.
9. Kivipelto, L., and Panula, P. (1991) Comparative distribution of neurons containing FLFQPQRFamide-like (morphine-modulating) peptide and related neuropeptides in the rat brain, *Eur. J. Neurosci. 3*, 175−185.
10. Espinoza, E., Carrigan, M., Thomas, S. G., Shaw, G., and Edison, A. S. (2000) A statistical view of FMRFamide neuropeptide diversity, *Mol. Neurobiol. 21*, 35−56.
11. Fisher, J. M., and Scheller, R. H. (1988) Prohormone processing and the secretory pathway, *J. Biol. Chem. 263*, 16515−16518.
12. Pascual, N., Castresana, J., Valero, M. L., Andreu, D., and Belles, X. (2004) Orcokinins in insects and other invertebrates, *Insect Biochem. Mol. Biol. 34*, 1141−1146.
13. Conlon, J. M. (2001) Evolution of the insulin molecule: Insights into structure−activity and phylogenetic relationships, *Peptides 22*, 1183−1193.
14. Edison, A. S., Messinger, L. A., and Stretton, A. O. (1997) afp-1: A gene encoding multiple transcripts of a new class of FMRFamide-like neuropeptides in the nematode *Ascaris suum*, *Peptides 18*, 929−935.
15. Cowden, C., Stretton, A. O., and Davis, R. E. (1989) AF1, a sequenced bioactive neuropeptide isolated from the nematode *Ascaris suum*, *Neuron 2*, 1465−1473.
16. Cowden, C., and Stretton, A. O. (1993) AF2, an *Ascaris* neuropeptide: Isolation, sequence, and bioactivity, *Peptides 14*, 423−430.
17. Sithigorngul, P., Cowden, C., Guastella, J., and Stretton, A. O. (1989) Generation of monoclonal antibodies against a nematode peptide extract: Another approach for identifying unknown neuropeptides, *J. Comput. Neurol. 284*, 389−397.
18. Cowden, C., Sithigorngul, P., Brackley, P., Guastella, J., and Stretton, A. O. (1993) Localization and differential expression of FMRFamide-like immunoreactivity in the nematode *Ascaris suum*, *J. Comp. Neurol. 333*, 455−468.
19. Cowden, C., and Stretton, A. O. (1995) Eight novel FMRFamide-like neuropeptides isolated from the nematode *Ascaris suum*, *Peptides 16*, 491−500.
20. Bowman, J. W., Friedman, A. R., Thompson, D. P., Ichhpurani, A. K., Kellman, M. F., Marks, N., Maule, A. G., and Geary, T. G. (1996) Structure−activity relationships of KNEFIRFamide (AF1), a nematode FMRFamide-related peptide, on *Ascaris suum* muscle, *Peptides 17*, 381−387.

21. Bowman, J. W., Winterrowd, C. A., Friedman, A. R., Thompson, D. P., Klein, R. D., Davis, J. P., Maule, A. G., Blair, K. L., and Geary, T. G. (1995) Nitric oxide mediates the inhibitory effects of SDPNFLRFamide, a nematode FMRFamide-related neuropeptide, in *Ascaris suum*, *J. Neurophysiol. 74*, 1880−1888.
22. Nathoo, A. N., Moeller, R. A., Westlund, B. A., and Hart, A. C. (2001) Identification of neuropeptide-like protein gene families in *Caenorhabditis elegans* and other species, *Proc. Natl. Acad. Sci. U.S.A. 98*, 14000−14005.
23. Husson, S. J., Clynen, E., Baggerman, G., de Loof, A., and Schoofs, L. (2005) Discovering neuropeptides in *Caenorhabditis elegans* by two-dimensional liquid chromatography and mass spectrometry, *Biochem. Biophys. Res. Commun. 335*, 76−86.
24. Rosoff, M. L., Doble, K. E., Price, D. A., and Li, C. (1993) The flp-1 propeptide is processed into multiple, highly similar FMRFamide-like peptides in *Caenorhabditis elegans*, *Peptides 14*, 331−338.
25. Marks, N. J., Shaw, C., Maule, A. G., Davis, J. P., Halton, D. W., Verhaert, P., Geary, T. G., and Thompson, D. P. (1995) Isolation of AF2 (KHEYLRFamide) from *Caenorhabditis elegans*: Evidence for the presence of more than one FMRFamide-related peptide-encoding gene, *Biochem. Biophys. Res. Commun. 217*, 845−851.
26. Marks, N. J., Maule, A. G., Geary, T. G., Thompson, D. P., Davis, J. P., Halton, D. W., Verhaert, P., and Shaw, C. (1997) APEASPFIRFamide, a novel FMRFamide-related decapeptide from *Caenorhabditis elegans*: Structure and myoactivity, *Biochem. Biophys. Res. Commun. 231*, 591−595.
27. Marks, N. J., Maule, A. G., Geary, T. G., Thompson, D. P., Li, C., Halton, D. W., and Shaw, C. (1998) KSAYMRFamide (PF3/AF8) is present in the free-living nematode, *Caenorhabditis elegans*, *Biochem. Biophys. Res. Commun. 248*, 422−425.
28. Mercier, A. J., Friedrich, R., and Boldt, M. (2003) Physiological functions of FMRFamide-like peptides (FLPs) in crustaceans, *Microsc. Res. Tech. 60*, 313−324.
29. Rastogi, R. K., D'Aniello, B., Pinelli, C., Fiorentino, M., Di Fiore, M. M., Di Meglio, M., and Iela, L. (2001) FMRFamide in the amphibian brain: A comprehensive survey, *Microsc. Res. Tech. 54*, 158−172.
30. Brownlee, D. J., and Fairweather, I. (1999) Exploring the neurotransmitter labyrinth in nematodes, *Trends Neurosci. 22*, 16−24.
31. Dockray, G. J. (2004) The expanding family of −RFamide peptides and their effects on feeding behaviour, *Exp. Physiol. 89*, 229−235.
32. Yang, H. Y., Fratta, W., Majane, E. A., and Costa, E. (1985) Isolation, sequencing, synthesis, and pharmacological characterization of two brain neuropeptides that modulate the action of morphine, *Proc. Natl. Acad. Sci. U.S.A. 82*, 7757−7761.
33. Waggoner, L. E., Hardaker, L. A., Golik, S., and Schafer, W. R. (2000) Effect of a neuropeptide gene on behavioral states in *Caenorhabditis elegans* egg-laying, *Genetics 154*, 1181−1192.
34. Nelson, L. S., Rosoff, M. L., and Li, C. (1998) Disruption of a neuropeptide gene, flp-1, causes multiple behavioral defects in *Caenorhabditis elegans*, *Science 281*, 1686−1690.
35. Rogers, C., Reale, V., Kim, K., Chatwin, H., Li, C., Evans, P., and de Bono, M. (2003) Inhibition of *Caenorhabditis elegans* social feeding by FMRFamide-related peptide activation of NPR-1, *Nat. Neurosci. 6*, 1178−1185.
36. Kubiak, T. M., Larsen, M. J., Nulf, S. C., Zantello, M. R., Burton, K. J., Bowman, J. W., Modric, T., and Lowery, D. E. (2003) Differential activation of "social" and "solitary" variants of the *Caenorhabditis elegans* G protein-coupled receptor NPR-1 by its cognate ligand AF9, *J. Biol. Chem. 278*, 33724−33729.
37. Mertens, I., Vandingenen, A., Meeusen, T., Janssen, T., Luyten, W., Nachman, R. J., de Loof, A., and Schoofs, L. (2004) Functional characterization of the putative orphan neuropeptide G-protein coupled receptor C26F1.6 in *Caenorhabditis elegans*, *FEBS Lett. 573*, 55−60.
38. Mertens, I., Meeusen, T., Janssen, T., Nachman, R., and Schoofs, L. (2005) Molecular characterization of two G protein-coupled receptor splice variants as FLP2 receptors in *Caenorhabditis elegans*, *Biochem. Biophys. Res. Commun. 330*, 967−974.
39. Kubiak, T. M., Larsen, M. J., Zantello, M. R., Bowman, J. W., Nulf, S. C., and Lowery, D. E. (2003) Functional annotation of the putative orphan *Caenorhabditis elegans* G-protein-coupled receptor C10C6.2 as a FLP15 peptide receptor, *J. Biol. Chem. 278*, 42115−42120.
40. Johnson, E. C., Bohn, L. M., Barak, L. S., Birse, R. T., Nassel, D. R., Caron, M. G., and Taghert, P. H. (2003) Identification of *Drosophila* neuropeptide receptors by G protein-coupled receptors−$\beta$-arrestin2 interactions, *J. Biol. Chem. 278*, 52172−52178.
41. Lingueglia, E., Champigny, G., Lazdunski, M., and Barbry, P. (1995) Cloning of the amiloride-sensitive FMRFamide peptide-gated sodium channel, *Nature 378*, 730−733.
42. Cottrell, G. A. (1997) The first peptide-gated ion channel, *J. Exp. Biol. 200*, 2377−2386.
43. Furukawa, Y., Miyawaki, Y., and Abe, G. (2005) Molecular cloning and functional characterization of the *Aplysia* FMRFamide-gated $Na^+$ channel, *Pflugers Arch*.
44. Xie, J., Price, M. P., Wemmie, J. A., Askwith, C. C., and Welsh, M. J. (2003) ASIC3 and ASIC1 mediate FMRFamide-related peptide enhancement of $H^+$-gated currents in cultured dorsal root ganglion neurons, *J. Neurophysiol. 89*, 2459−2465.
45. Edison, A. S., Espinoza, E., and Zachariah, C. (1999) Conformational ensembles: The role of neuropeptide structures in receptor binding, *J. Neurosci. 19*, 6318−6326.
46. Andersen, N. H., Neidigh, J. W., Harris, S. M., Lee, G. M., Liu, Z., and Tong, H. (1997) Extracting information from the temperature gradients of polypeptide NH chemical shifts. 1. The importance of conformational averaging, *J. Am. Chem. Soc. 119*, 8547−8561.
47. Silverman, S. K., Lester, H. A., and Dougherty, D. A. (1996) Subunit stoichiometry of a heteromultimeric G protein-coupled inward-rectifier $K^+$ channel, *J. Biol. Chem. 271*, 30524−30528.
48. van Renterghem, C., Bilbe, G., Moss, S., Smart, T. G., Constanti, A., Brown, D. A., and Barnard, E. A. (1987) GABA receptors induced in *Xenopus* oocytes by chick brain mRNA: Evaluation of TBPS as a use-dependent channel-blocker, *Brain Res. 388*, 21−31.
49. Brown, N. A., McAllister, G., Weinberg, D., Milligan, G., and Seabrook, G. R. (1995) Involvement of G-protein α il subunits in activation of G-protein gated inward rectifying $K^+$ channels (GIRK1) by human NPY1 receptors, *Br. J. Pharmacol. 116*, 2346−2348.
50. Reale, V., Hannan, F., Hall, L. M., and Evans, P. D. (1997) Agonist-specific coupling of a cloned *Drosophila melanogaster* D1-like dopamine receptor to multiple second messenger pathways by synthetic agonists, *J. Neurosci. 17*, 6545−6453.
51. Piotto, M., Saudek, V., and Sklenar, V. (1992) Gradient-tailored excitation for single-quantum NMR spectroscopy of aqueous solutions, *J. Biomol. NMR 2*, 661−665.
52. Schweiger, A., Braunschweiler, L., Fauth, J., and Ernst, R. R. (1985) Coherent and incoherent echo spectroscopy with extended-time excitation, *Phys. Rev. Lett. 54*, 1241−1244.
53. Bothner-By, A. A., Stephens, R. L., Lee, J., Warren, C. D., and Jeanloz, R. W. (1984) Structure determination of a tetrasaccharide: Transient nuclear Overhauser effects in the rotating frame, *J. Am. Chem. Soc. 106*, 811−813.
54. Delaglio, F., Grzesiek, S., Vuister, G. W., Zhu, G., Pfeifer, J., and Bax, A. (1995) NMRPipe: A multidimensional spectral processing system based on UNIX pipes, *J. Biomol. NMR 6*, 277−293.
55. Johnson BA, B. R. (1994) a computer program for the visualization and analysis of NMR data, *J. Biomol. NMR 4*, 603−614.
56. Wuthrich, K. (1986) *NMR of Proteins and Nucleic Acids*, John Wiley and Sons, New York.
57. Betz, M., Lohr, F., Wienk, H., and Ruterjans, H. (2004) Long-range nature of the interactions between titratable groups in *Bacillus agaradhaerens* family 11 xylanase: pH titration of *B. agaradhaerens* xylanase, *Biochemistry 43*, 5820−5831.
58. Carlacci, L., and Edison, A. S. (2000) Computational analysis of two similar neuropeptides yields distinct conformational ensembles, *Proteins 40*, 367−377.
59. Stretton, A. O., Cowden, C., Sithigorngul, P., and Davis, R. E. (1991) Neuropeptides in the nematode *Ascaris suum*, *Parasitology 102* (supplement), S107−S116.
60. Payza, K., Greenberg, M. J., and Price, D. A. (1989) Further characterization of Helix FMRFamide receptors: Kinetics, tissue distribution, and interactions with the endogenous heptapeptides, *Peptides 10*, 657−661.
61. Marqusee, S., Robbins, V. H., and Baldwin, R. L. (1989) Unusually stable helix formation in short alanine-based peptides, *Proc. Natl. Acad. Sci. U.S.A. 86*, 5286−2590.

62. Chakrabartty, A., Kortemme, T., and Baldwin, R. L. (1994) Helix propensities of the amino acids measured in alanine-based peptides without helix-stabilizing side-chain interactions, *Protein Sci. 3*, 843−852.
63. Wishart, D. S., Sykes, B. D., and Richards, F. M. (1991) Relationship between nuclear magnetic resonance chemical shift and protein secondary structure, *J. Mol. Biol. 222*, 311−333.
64. Schwarzinger, S., Kroon, G. J., Foss, T. R., Wright, P. E., and Dyson, H. J. (2000) Random coil chemical shifts in acidic 8 M urea: Implementation of random coil shift data in NMRView, *J. Biomol. NMR 18*, 43−48.
65. Schwarzinger, S., Kroon, G. J., Foss, T. R., Chung, J., Wright, P. E., and Dyson, H. J. (2001) Sequence-dependent correction of random coil NMR chemical shifts, *J. Am. Chem. Soc. 123*, 2970−2978.
66. Wishart, D. S., and Case, D. A. (2001) Use of chemical shifts in macromolecular structure determination, *Methods Enzymol. 338*, 3−34.
67. Lin, J. C., Barua, B., and Andersen, N. H. (2004) The helical alanine controversy: An (Ala)6 insertion dramatically increases helicity, *J. Am. Chem. Soc. 126*, 13679−13684.
68. Andersen, N. H., Cao, B., and Chen, C. (1992) Peptide/protein structure analysis using the chemical shift index method: Upfield α-CH values reveal dynamic helices and α L sites, *Biochem. Biophys. Res. Commun. 184*, 1008−1014.
69. Dyson, H. J., Rance, M., Houghten, R. A., Lerner, R. A., and Wright, P. E. (1988) Folding of immunogenic peptide fragments of proteins in water solution. I. Sequence requirements for the formation of a reverse turn, *J. Mol. Biol. 201*, 161−200.
70. Dyson, H. J., Rance, M., Houghten, R. A., Wright, P. E., and Lerner, R. A. (1988) Folding of immunogenic peptide fragments of proteins in water solution. II. The nascent helix, *J. Mol. Biol. 201*, 201−217.
71. Blanco, F. J., Serrano, L., and Forman-Kay, J. D. (1998) High populations of non-native structures in the denatured state are compatible with the formation of the native folded state, *J. Mol. Biol. 284*, 1153−1164.
72. Osterhout, J. J., Jr., Baldwin, R. L., York, E. J., Stewart, J. M., Dyson, H. J., and Wright, P. E. (1989) $^1$H NMR studies of the solution conformations of an analogue of the C-peptide of ribonuclease A, *Biochemistry 28*, 7059−7064.
73. Bundi, A., and Wuthrich, K. (1977) $^1$H NMR titration shifts of amide proton resonances in polypeptide chains, *FEBS Lett. 77*, 11−14.
74. Bundi, A., Wuthrich, K. (1979) Use of $^1$H-NMR titration shifts for studies of polypeptide conformation, *Biopolymers 18*, 299−311.
75. Szyperski, T., Antuch, W., Schick, M., Betz, A., Stone, S. R., and Wuthrich, K. (1994) Transient hydrogen bonds identified on the surface of the NMR solution structure of Hirudin, *Biochemistry 33*, 9303−9310.
76. Baxter, N. J., and Williamson, M. P. (1997) Temperature dependence of $^1$H chemical shifts in proteins, *J. Biomol. NMR 9*, 359−369.
77. Silva, M. V., Elipe, R. T. M., Bednarek, M. A., Arison, B. H. (2003) $^1$H-NMR studies on a potent and selective antagonist at human melanocortin receptor 4 (hMC-4R), *Biopolymers 68*, 512−527.
78. Higashijima, T., Tasumi, M., and Miyazawa, T. (1975) H nuclear magnetic resonance studies of melanostatin: Dependence of the chemical shifts of NH protons on temperature and concentration, *FEBS Lett. 57*, 175−178.
79. Kenakin, T. (2004) Principles: Receptor theory in pharmacology, *Trends Pharmacol. Sci. 25*, 186−192.
80. Evans, P. D., Robb, S., Cheek, T. R., Reale, V., Hannan, F. L., Swales, L. S., Hall, L. M., and Midgley, J. M. (1995) Agonist-specific coupling of G-protein-coupled receptors to second-messenger systems, *Prog. Brain Res. 106*, 259−268.
81. Robb, S., Cheek, T. R., Hannan, F. L., Hall, L. M., Midgley, J. M., and Evans, P. D. (1994) Agonist-specific coupling of a cloned *Drosophila* octopamine/tyramine receptor to multiple second messenger systems, *EMBO J. 13*, 1325−1330.
82. Spengler, D., Waeber, C., Pantaloni, C., Holsboer, F., Bockaert, J., Seeburg, P. H., and Journot, L. (1993) Differential signal transduction by five splice variants of the PACAP receptor, *Nature 365*, 170−175.
83. Floyd, P. D., Li, L., Rubakhin, S. S., Sweedler, J. V., Horn, C. C., Kupfermann, I., Alexeeva, V. Y., Ellis, T. A., Dembrow, N. C., Weiss, K. R., and Vilim, F. S. (1999) Insulin prohormone processing, distribution, and relation to metabolism in *Aplysia californica*, *J. Neurosci. 19*, 7732−7741.
84. Li, L., Moroz, T. P., Garden, R. W., Floyd, P. D., Weiss, K. R., and Sweedler, J. V. (1998) Mass spectrometric survey of interganglionically transported peptides in *Aplysia*, *Peptides 19*, 1425−1433.

BI0603928